

Andrzej POSMYK*

TRIBOLOGICAL PROPERTIES OF PISTON RINGS DESIGNED FOR SLIDING AGAINST COMPOSITE MATERIALS IN LUBRICATED CONTACTS

WŁAŚCIWOŚCI TRIBOLOGICZNE PIERŚCIENI TŁOKOWYCH PRZEZNACZONYCH DO WSPÓŁPRACY Z MATERIAŁAMI KOMPOZYTOWYMI W SMAROWANYCH SKOJARZENIACH

Key words:

means of transport, piston rings, composite materials, ceramic particles, chromium coating.

Abstract:

The paper presents basic information on the production, structure and tribological properties of a composite chromium-ceramic coating deposited electrolytically on a cast-iron piston ring for a combustion engine designed for sliding against a composite cylinder liner. The results of comparative tests of two contacts, i.e. cast-iron GJL-250/AlMC and GJL250+Cr-Al₂O₃/AlMC, are described. The deposition of the Cr-Al₂O₃ coating on the cast-iron piston ring reduces almost threefold the wear of the piston ring and about 20% the friction resistance in the contact due to the presence of aluminium oxide particles and fibres. The reinforcing phase removed from the chromium layer polishes the chromium and composite sliding surfaces. The places left by the removed particles serve as depots for oil, which reduces the friction forces and minimises oil consumption. The Al₂O₃ wear debris decreases the roughness of the surfaces in contact, which additionally reduces the friction forces according to the friction hypothesis of Ernst and Merchant.

Słowa kluczowe:

środki transportu, pierścienie tłokowe, materiały kompozytowe, cząstki ceramiczne, powłoka chromowa.

Streszczenie:

W artykule opisano podstawy wytwarzania, budowę i właściwości tribologiczne kompozytowej powłoki chromowo-ceramicznej naniesionej elektrolitycznie na żeliwny pierścień tłokowy silnika spalinowego przeznaczony do współpracy z kompozytową tuleją cylindrową. Opisano wyniki badań porównawczych dwóch skojarzeń, tj. żeliwa GJL-250/AlMC i GJL-250+Cr-Al₂O₃/AlMC. Naniesienie powłoki Cr-Al₂O₃ na pierścień żeliwny zmniejsza ponad trzykrotnie zużycie pierścienia i około 20% opory tarcia skojarzenia dzięki obecności cząstek i włókien tlenku aluminium. Usunięta z chromu faza zbrojąca działa polerująco na współpracujące powierzchnie chromu i kompozytu. Miejsca po usuniętych cząstkach służą do gromadzenia oleju, co zmniejsza siły tarcia i zużycie oleju. Produkty zużycia Al₂O₃ zmniejszają chropowatość współpracujących powierzchni, co dodatkowo zmniejsza siły tarcia zgodnie z hipotezą tarcia Ernsta i Merchanta.

INTRODUCTION

For many years, university research centres dealing with materials engineering and tribology and many factories have been devoting increasingly more time to the design, production, investigation and application of composite materials in the construction of technical means of transport [L. 1, 2]. The benefits of using composite materials result mainly from three of their basic properties, i.e.

- increasing the strength of composites when compared to the matrix (in wrought alloys up to 30% and in cast alloys to 40%),
- lowering friction forces and wear (several times) by improving lubrication resulting from the biplanar nature of the composite surface layer (the reinforcing phase protrudes above the matrix surface as a result of the large difference in the hardness of the matrix and reinforcing phase, from fractions of a micrometre to several micrometres, Fig. 1),

* ORCID: 0000-0003-2943-2379. Silesian University of Technology Faculty of Transport and Aviation Engineering, Krasińskiego 8 Street, 40-019 Katowice, Poland.

- increasing the thermal conductivity, e.g. in brake discs after adding SiC, for which $\lambda = 100 - 300 \text{ W}/(\text{m}\cdot\text{K})$, at $\lambda = 130 - 160 \text{ W}/(\text{m}\cdot\text{K})$ for the matrix material made of silumin,
- diminishing the thermal expansion to reduce the montage clearance of the engine piston up to 10% [L. 2].

Thanks to the use of composites, it is possible to reduce the weight of vehicles, their fuel consumption, and the quantity of pollution they emit. This is of particular importance in automotive and aviation transport. The composites used in the construction of the Boeing Dreamliner have reduced its fuel consumption by 30% and even

more in the Airbus A350F. The weight of trains in the USA (Amtrak) has been reduced by almost 12 tons owing to composite brake discs. Many works dedicated to metal, ceramic and polymer composites used in short- and long-distance transport can be found in the literature. In many papers, information about the production of AIMCs, their properties and applications can be found.

In practically most publications [L. 3–4] information can be found on raising the wear resistance of the matrix material by increasing the reinforcing phase (RP) content and extending the durability of vehicle components made of composites as a consequence of less wear.

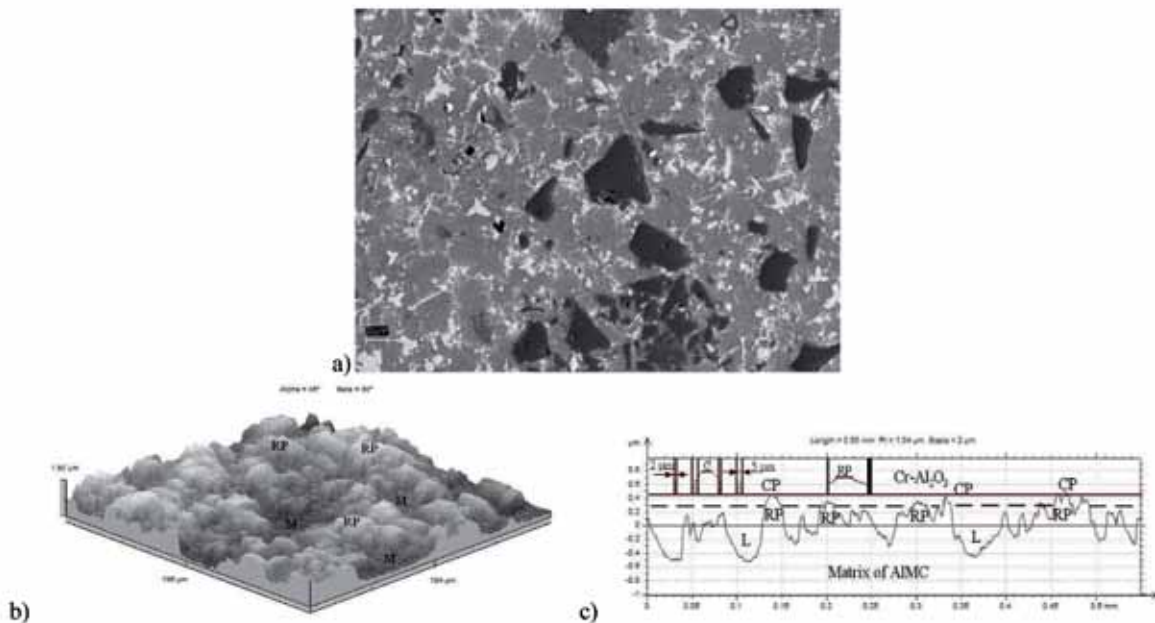


Fig. 1. Surface of cylinder sleeve made of composite with Al_2O_3 particles with a diameter of $15 \mu\text{m}$ (a) before sliding, 3D (b) and 2D (c) roughness profile during sliding against $\text{Cr-Al}_2\text{O}_3$ coating: M – matrix, RP – reinforcing particles, CIP – contact point, L – lubricant, C – cavities after removal of reinforcing phase, filled with oil

Rys. 1. Powierzchnia tulei cylindrowej wykonanej z kompozytu z cząstkami Al_2O_3 o średnicy $15 \mu\text{m}$ (a) przed współpracą ślizgową oraz profile chropowatości 3D (b) i 2D (c) podczas współpracy z powłoką $\text{Cr-Al}_2\text{O}_3$: M – osnowa, RP – cząstki zbrojące, CP – punkt styku, L – smar, C – przestrzeń po wykruszonej fazie zbrojącej wypełnione olejem

Less space, or even none at all, is devoted to the partner sliding against the produced and studied composites. This is very important because the cast iron piston rings slide on the composite surface of the combustion engine cylinder liner, whose wear, not only that of the sleeve, significantly impacts the engine's durability. The gap between them decides the compression ratio, engine efficiency, and the amount of emitted pollutants. The presence

of a hard reinforcing phase (Vickers hardness $14-17 \text{ GPa}$ for Al_2O_3 ; 25 GPa for SiC [L. 5]) in the cylinder sleeve increases the wear of the piston rings ($180-240 \text{ HB}$ or $192-253 \text{ HV}$ for GJL-150).

The author's own research [L. 6] and a few other authors show that the presence of an RP, most often ceramic (Al_2O_3 , SiC) in the form of fibres or particles, dramatically changes the conditions in sliding contacts. Depending on the stereological

features of the RP, such as the surface fraction (NA), average particle diameter (d), shape ratio (ξ) and the chemical composition (Al_2O_3 , SiC, glassy carbon, mica), the stresses and strains change in the contact zone of the partner sliding against the composite. In unfavourable cases (e.g. a large diameter of the reinforcing phase particles), local stresses occur that exceed the value of stresses permissible for given materials, and the accompanying local deformations contribute to the growth in friction resistance and excessive wear of the partner [L. 8].

Appreciating the importance of this problem, some centres began to develop new materials and already-known research from other applications intended for sliding against composites containing a ceramic reinforcing phase. The piston rings of internal combustion engines are cast iron with lamellar and spheroidal graphite, steel, and stainless steel.

New technologies were also developed to protect the previously used materials against excessive wear sliding against composites [L. 9–11]. Piston rings are covered with chromium, molybdenum, phosphate and nitride coatings. One of the earlier solutions known from diesel engines [L. 12], is the covering of cast iron piston rings with composite coatings (CKS) sliding against a cast iron cylinder liner or a cast iron sleeve covered with hard chromium [L. 9, 13], which extends their durability up to several times. This coating consists of chromium, dispersed particles (diameter 2–5 μm), and short aluminium oxide fibres (diameter 2–3 μm). Since 2004, composite coatings (GDC) with a diamond reinforcing phase, containing synthetic diamond particles with an average diameter of 0.5 μm , have been used in lorries [L. 9]. The wear of the rings covered with this coating is about four times lower than the chromium coating and two times lower than the chromium-ceramic coating. For sliding against a chromium-plated (th. 30 μm , 700 HV0.1) cast iron sleeve, when lubricated with oils containing diamond nanoparticle additives, Cr plated, and nitrided rings (CrN – 1100 HV0.1) are also used [L. 14]. In the combustion engine manufacturing community, such rings are sometimes referred to as ceramic rings.

In 2012, diamond-like carbon coatings with a thickness of up to 25 μm (5000 HV0.2) were introduced, reducing ring friction forces to 100 N in a cylinder liner with a diameter of 130 mm (Euro 6 requirements). In the next stage of the

development of composite coatings, nanoparticles were used, e.g. mixtures of cerium (CeO_2) and cerium compounds with an addition of yttrium (8YDC) deposited in a nickel coating. However, the dimensions of the nanoparticles (8–28 nm) and agglomerates (2.6 μm) or stronger adhesion to Ni do not reduce friction forces (μ 0.5–0.7) as well as the Cr- Al_2O_3 coating [L. 15].

The reinforcing phase in the composite coating with a hard chromium matrix plays a slightly different role. Al_2O_3 particles and fibres crumble to form reservoirs for oil (C in Fig. 1d) with a 2–5 μm diameter. Their wear products reach the friction surfaces, reducing their roughness and friction resistance.

The presented short analysis of the applications of chromium-ceramic coatings shows that, to date, they have been employed as protection against the intensive wear of cast iron sliding against cast iron or steel sleeves covered with chromium, nickel and composite coatings with a Cr or Ni matrix.

It is difficult to find information on the applications of these coatings for sliding against composites containing ceramic particles or reinforcing fibres, which intensify the wear of the sliding partner cooperating with containing them.

This article describes the results of an attempt to use cast iron rings covered with a chromium-ceramic (Cr- Al_2O_3) composite coating for cooperation with composites based on aluminium alloys in conditions of limited lubrication, which can reduce the emission of pollutants by technical means of transport powered by internal combustion engines.

THEORETICAL BASES OF PRODUCING MATERIALS TO SLIDE AGAINST COMPOSITES

The hypothesis of friction developed by Ernst and Merchant [L. 16] (Formula 1) shows that the appropriate selection of materials can shape the coefficient of sliding friction. There should be one material with low shear strength (τ) and one with high hardness in the contact.

$$\mu = \tau/\text{HB} + \text{tg} \quad (1)$$

The roughness of the surfaces of the sliding parts should be small ($\text{tg}\alpha$ in Formula 1), i.e. the angle of inclination of the peaks of the surface irregularities should be small. A polished piston

ring with a chromium-ceramic composite coating sliding against a silumin matrix composite containing very hard Al_2O_3 particles or fibres and a low shear strength oil can provide low wear. Acting as a polishing paste, the fibres and Al_2O_3 particles present in the entire volume of the coating contribute to the continuous run-in of the sliding surfaces and the reduction of friction forces. If we use limited lubrication (a reduced amount of oil fed to the friction zone) in this contact, the emission of harmful oil combustion products will also be reduced.

From the tribological point of view, the presence of hard chromium on the surface of the ring with evenly distributed Al_2O_3 particles and fibres, as well as the content of Al_2O_3 fibres or particles in the cylinder liner surface (**Fig. 1b**), will ensure minimal wear of the surface and oil.

Oils and greases are quickly removed from the friction zone by the mutually moving parts, e.g. the engine oil ring. To ensure the constant presence of oil in the friction zone, it should be "anchored" to the surfaces of the sliding parts. In the discussed composite coating, oil reservoirs are created in places left by ceramic particles and fibres crushed during friction (**Fig. 2**). In the contact of a ring covered with the $\text{Cr-Al}_2\text{O}_3$ coating with the composite cylinder sleeve, there are additional oil reservoirs resulting from the biplanar nature of the composite as a result of the protrusion of RP above the surface of the matrix (**Fig. 1b** and **1c**). These reservoirs make it possible to reduce the amount of oil fed to the contact, which reduces operating costs and environmental pollution. The wear products of the short oxide fibres serve as a polishing material for the contact surfaces, which reduces the roughness and coefficient of friction.

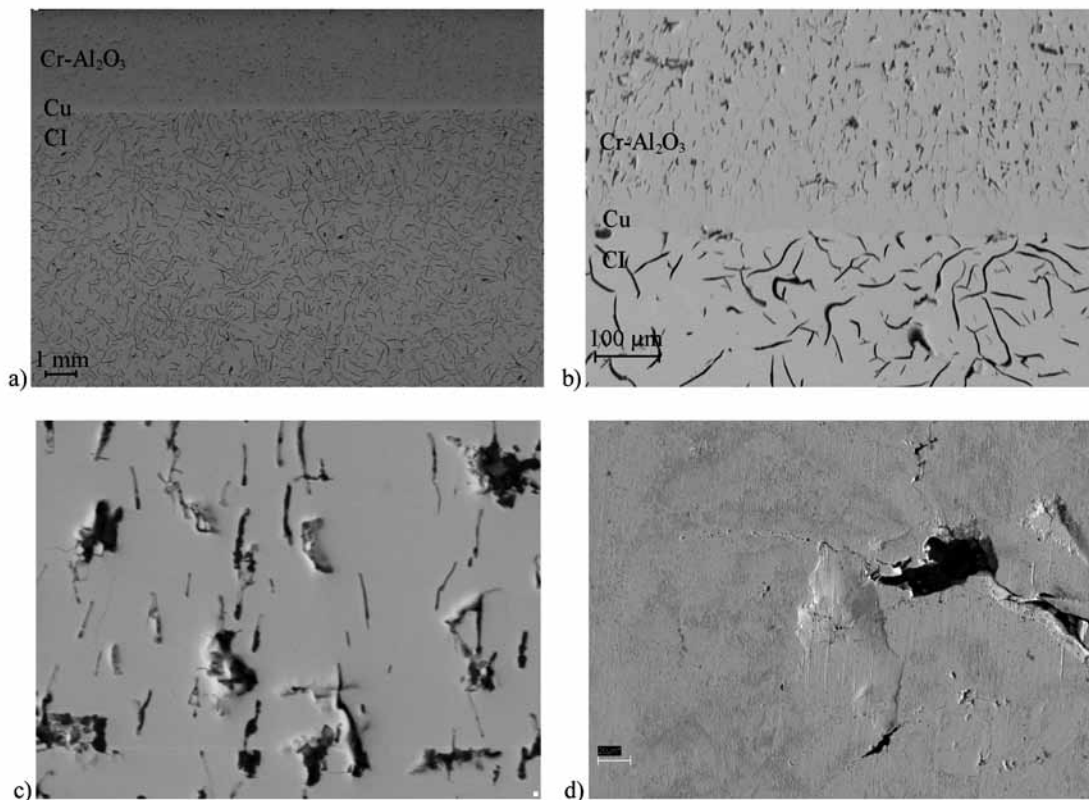


Fig. 2. Piston ring with Cr coating with Al_2O_3 particles and fibres; SEM: a – polished cross-section with visible cast iron (CI), Cu interlayer and $\text{Cr-Al}_2\text{O}_3$ coating; b – Cu transition layer between cast iron and coating increasing adhesion of Cr; c – friction surface of $\text{Cr-Al}_2\text{O}_3$ – coating before sliding – visible areas after removed Al_2O_3 fibres and particles; d – a magnified fragment of the cavity after removed RP functioning as a lubricant reservoir

Rys. 2. Pierścień żeliwny pokryty powłoką chromową z cząstkami i włóknami Al_2O_3 ; SEM: a – zgląd z widocznym żelazem (CI), międzywarstwą Cu i powłoką $\text{Cr-Al}_2\text{O}_3$; b – warstwa przejściowa z Cu pomiędzy żelazem i powłoką zwiększająca przyczepność Cr; c – powierzchnia robocza powłoki $\text{Cr-Al}_2\text{O}_3$ przed współpracą ślizgową – widoczne miejsca po usuniętych włóknach i cząstkach Al_2O_3 ; d – powiększony fragment wgłębienia po wykruszonym Al_2O_3 , stanowiącego zasobnik środka smarnego

SELECTED PROPERTIES OF MATERIALS FOR SLIDING AGAINST COMPOSITES

When two hard materials slide against each other, a third body with low shear strength is needed. In most lubricated contacts, it is the lubricant. To ensure low friction resistance, a lubricant film is needed to separate the protrusions of the unevenness of the sliding bodies. It is known from practice that not all engineering materials allow a film of lubricant to be maintained on them. A classic example is chromium, on the surface of which it is difficult to sorb oils. In the contact of a cast iron ring covered with a layer of chromium with a composite containing Al_2O_3 particles or

fibres, it is difficult to create an oil film; therefore, the developed chromium coatings modified with aluminium oxide particles and fibres can be used.

A copper interlayer is deposited on the cast iron, increasing chromium adhesion to the cast iron. The Cr- Al_2O_3 method produces the electrolytic coating with the alternating polarisation of the electrodes. When cast iron is connected to a negative pole of the current source, chromium ions are deposited on it, and after changing the polarity, the polarised Al_2O_3 particles and fibres are incorporated into the chromium. The effects of the polarisation change can be seen in the multiple layers exposed after the coating is etched (**Fig. 3**).

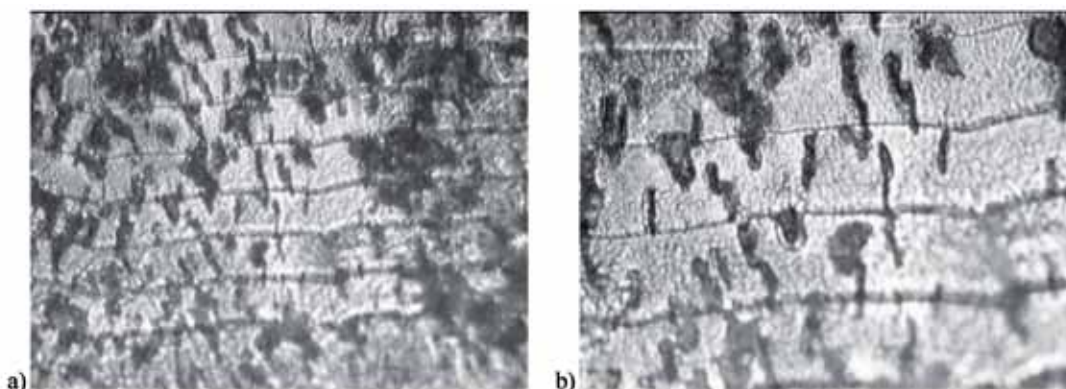


Fig. 3. Surface of a polished cross-section of composite Cr- Al_2O_3 coating electrolytically deposited on cast iron piston ring; chromium layers reinforced with Al_2O_3 (two-stages etching in 10% NaOH+10%HCl aqueous solution, visible Cr layers and dark Al_2O_3 inclusions)

Rys. 3. Powierzchnia zglądu poprzecznego wytworzonej elektrolitycznie na pierścieniu żeliwnym kompozytywnej powłoki chromowo-ceramicznej; warstwy chromu zbrojone Al_2O_3 (trawione dwuetapowo w 10% wodnym roztworze NaOH+10% HCl, wyraźnie widoczne warstwy Cr i ciemne wtrącenia Al_2O_3)

The task of the Al_2O_3 particles is to chip during sliding and create reservoirs for the lubricant (**Fig. 2c, 2d**). At the same time, the oxide chipped and fragmented due to friction, facilitates run-in of the sliding surfaces, which decreases their roughness and coefficient of friction. The view and cross-section of the sliding surface of the ring covered with the Cr- Al_2O_3 coating, designed for sliding contact, are shown in **Figures 2 and 3**.

CONDITIONS AND COURSE OF TESTS

Comparative tests of the discussed materials were carried out on a tribological testing machine (**Fig. 4**), the contact of which reproduces the operation of the piston group, i.e. the rings and the

cylinder liner surface or the piston skirt and the cylinder liner in conditions of limited lubrication [**L. 2, 8**]. These conditions are similar to the cold start of an internal combustion engine. The sample consists of sectors of the piston ring or piston skirt and the counter-sample of sectors along the generating line of the cylinder sleeve (**Fig. 5**). The contact is lubricated with oil mist supplied by the system, which gives the possibility to control the type of oil used (the injection conditions are adjusted to the viscosity), injection frequency and dose size.

Samples in the form of cuboids (10x10x13) were cut out from a piston ring with a working surface covered with a Cr- Al_2O_3 coating. Counter-samples in the form of a cuboid (65x15x8) were made of the AlSi12NiMgCu (AC-47000) composite

reinforced with 15% Al_2O_3 particles and cut out of the cylinder sleeve (marked as AIMC in Fig 6). The test was conducted under the following conditions:

- relative velocity: $v = 2.5$ m/s,
- unit pressure: $p = 3$ MPa,
- friction: lubrication with Lotos Synthetic oil (5W/40), oil dose approx. 2 mg every 30 min,
- test time: $t = 5 \times 10$ h in 4 repetitions,
- samples: cast iron ring with a chrome-ceramic coating (GJL-250+Cr- Al_2O_3),
- counter-samples: investigated composite AC-47000+15% Al_2O_3

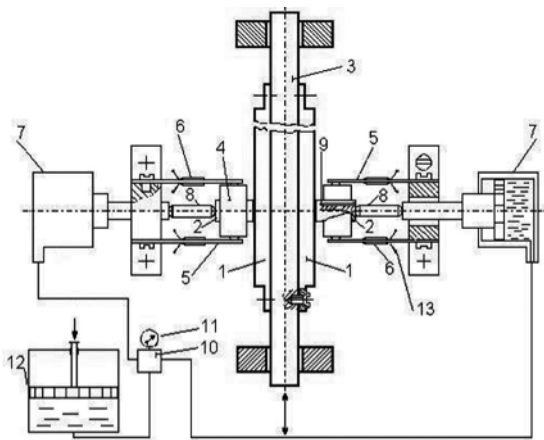


Fig. 4. Diagram of tribological tester: 1 – counter-sample, 2 – sample, 3 – guide, 4 – articulated sample holder, 5 – force transducer, 6 – strain gauge bridge, 7 – hydraulic cylinder, 8 – articulated pusher, 9 – hole for thermocouple, 10 – 4/2 manipulator, 11 – pressure gauge, 12 – hydraulic pump, 13 – output to Spider 4

Rys. 4. Schemat testera tribologicznego: 1 – przeciwpróbka, 2 – próbka, 3 – prowadnica, 4 – przegubowy uchwyt próbki, 5 – przetwornik siły, 6 – mostek tensometryczny, 7 – siłownik hydrauliczny, 8 – przegubowy popychacz, 9 – otwór pod termoparę, 10 – rozdzielacz 4/2, 11 – ciśnieniomierz, 12 – pompa hydrauliczna, 13 – wyjście do rejestratora Spider 4

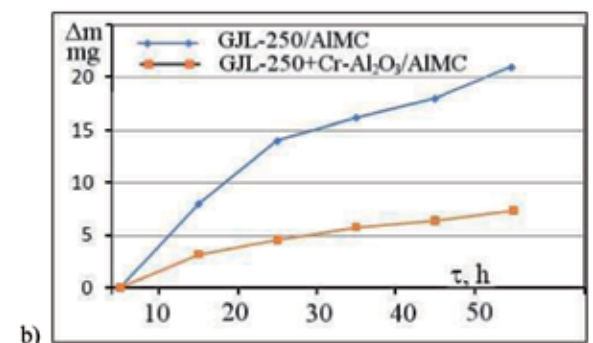
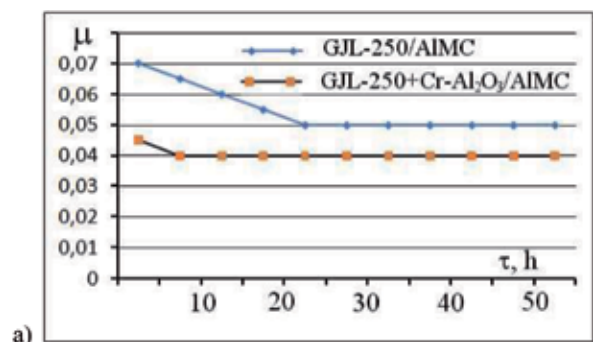


Fig. 5. Sample – GJL-250+Cr- Al_2O_3 (top) and counter-sample AC-47000+15% Al_2O_3 (bottom) after tribological tests

Rys. 5. Próbkę – GJL-250+Cr- Al_2O_3 (góra), i przeciwpróbka AC-47000+15% Al_2O_3 (dół) po badaniach tribologicznych

TESTS RESULTS

During the tests, the weight losses (Δm) of the samples and counter-samples, as well as the coefficient of friction (μ), were measured. The obtained results are presented in Fig. 6. Equations describing the dependence of the sample weight losses and coefficient of friction as a function of the sliding time (τ) as well as the values of the correlation coefficients (R), significance coefficients (α) and standard deviations ($\sigma_{\Delta m}$, σ_{μ}) of the equations from the measurement results are given below the graphs.



$$\begin{aligned} \mu_{\text{GJL-250}} &= 0.00001\tau^2 - 0.001\tau + 0.0699 & \Delta m_{\text{GJL-250}} &= -0.016\tau^2 + 1.42\tau - 11.6 \\ \alpha &= 0.08; R=0.96; \sigma_{\mu} &= 0.05 & \Delta m_{\text{Cr-Al}_2\text{O}_3} &= -0.006\tau^2 + 0.5\tau - 4 \\ \mu_{\text{Cr-Al}_2\text{O}_3} &= 0.0045\tau^3 + 0.11\tau^2 - 0.75\tau + 0.32 & \alpha &= 0.05; R=0.98; \sigma_{\Delta m} &= 0.83 \\ \alpha &= 0.05; R=0.98; \sigma_{\mu} &= 0.0005 & & \end{aligned}$$

Fig. 6. Dependences of coefficient of friction (a) and mass decrease (b) on sliding time (τ) in GJL-250/AIMC and GJL-250+Cr- Al_2O_3 /AIMC contacts lubricated with oil mist 2 mg/cm² every 30 min, $p = 3$ MPa, $v = 2.5$ m/s)

Rys. 6. Zależności współczynnika tarcia (a) i ubytku masy próbek (b) od czasu współpracy (τ) w skojarzeniach GJL-250/AIMC i GJL-250+Cr- Al_2O_3 /AIMC smarowane mgłą olejową 2 mg/cm² co 30 min, $p = 3$ MPa, $v = 2,5$ m/s)

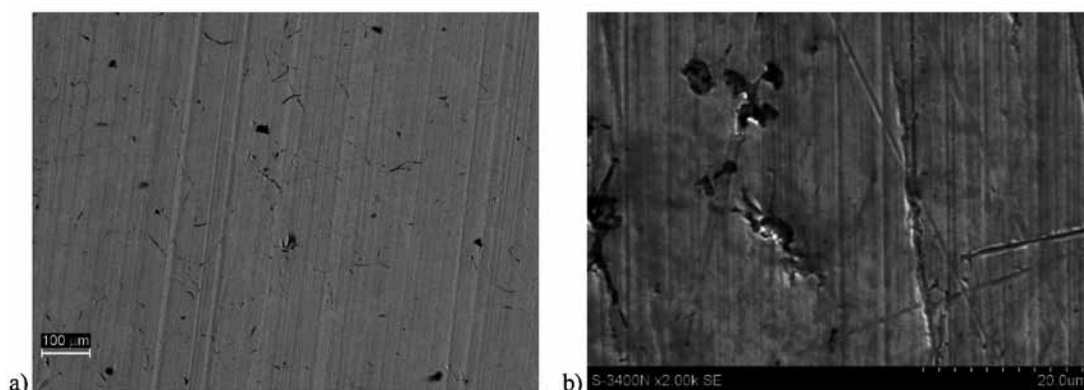


Fig. 7. Piston ring surface made of EN GJL-250 (a) and GJL-250 coated with Cr-Al₂O₃ layer (b) after sliding against composite including Al₂O₃ particles with a diameter of 15 μm (b) – visible traces of abrasion wear along the direction of movement ($p = 3 \text{ MPa}$, $v = 2.5 \text{ m/s}$)

Rys. 7. Widok powierzchni pierścienia z żeliwa EN GJL-250 (a) i GJL-250 pokrytego powłoką Cr-Al₂O₃ po współpracy z kompozytem zawierającym cząstki Al₂O₃ o średnicy 15 μm – widoczne ślady zużycia ściernego wzdłuż kierunku ruchu ($p = 3 \text{ MPa}$, $v = 2,5 \text{ m/s}$)

The surfaces of the samples after the tribological tests were investigated utilising a Hitachi S-4200 scanning microscope. At selected points of the friction surface of the samples with the composite coatings, the chemical composition was analysed using the SEM equipped with an EDS phase composition analysis device. The results are presented in **Figs. 7–9**. **Fig. 7a** shows the surface of the cast iron sample, and **Fig. 7b** displays the surface of the cast iron sample with the composite coating.

DISCUSSION OF RESULTS

Fig. 7a shows mild abrasive wear (scratches along the direction of movement) of the cast iron surface by protruding Al₂O₃ particles and hard silicon precipitates (bright Si-grains in **Fig. 1a**) that dominated the contact. Wear exposed flakes of graphite. In contact with the composite coating, abrasive wear was also dominant but less intense – almost three times lower after 50 hours of cooperation (**Fig. 6b**). In order to show the scratches from abrasive wear, a photograph with 5.5 times magnification was used (**Fig. 7b**).

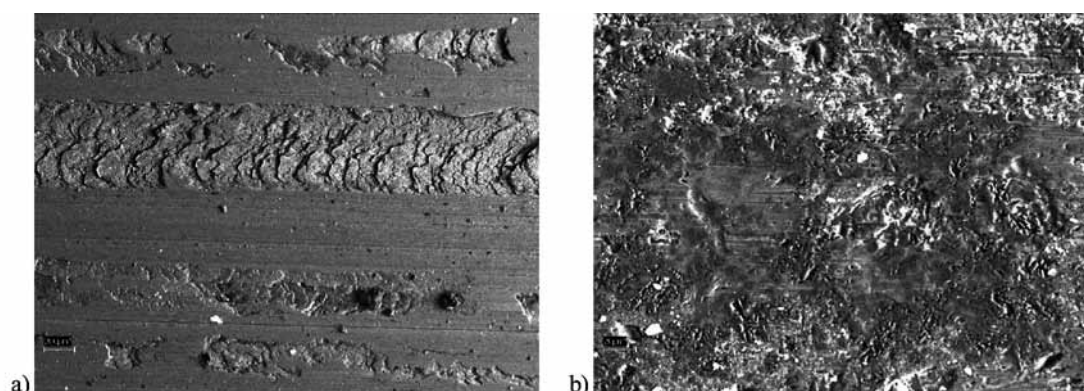


Fig. 8. Composite surface containing reinforcing particles 15 μm in diameter after sliding against piston ring GJL-250 (a) and GJL-250+ Cr-Al₂O₃ (b)

Rys. 8. Widok powierzchni kompozytu z cząstkami o średnicy 15 μm (a) po współpracy z pierścieniem GJL-250 (a) i GJL-250+ Cr-Al₂O₃ (b)

Figure 9a shows points (1–4) where qualitative and quantitative analyses of selected elements were performed. The first point is a continuous chromium coating without a ceramic reinforcing phase (Cr peaks in **Fig. 9b**). At Point 2, Cr surrounds an Al_2O_3 particle. It was exposed due to wear of the chromium layer, as shown in **Fig. 7b**. This is confirmed by the Al and O peaks in **Fig. 9c**. Chromium wear products were deposited on the Al_2O_3 particle, as indicated by the Cr peaks. At Point 3, an Al_2O_3 fibre emerges from the Cr layer, with an Al_2O_3 particle next to it (shown in **Fig. 7b**), which is confirmed by the Al, O and Cr peaks (**Fig. 9c**). At Point 4, Al_2O_3 emerges from under the Cr layer (**Fig. 9d**).

The value of the coefficient of friction in contact with the composite coating (GJL-250+Cr- Al_2O_3 /AIMC) did not exceed 0.04 after running in with a small amount of oil of 2 mg/cm^2 applied every 30 minutes. The worn aluminium

oxide mixed with oil was a good lubricating and polishing substance, which facilitated the running-in of the contact, as evidenced by the stabilisation of both the coefficient of friction and wear after about 10 hours of sliding. In the contact without the coating (GJL-250/AIMC), the coefficient of friction stabilised at a higher level ($\mu = 0.05$) after about 25 h of sliding.

Greater friction forces in contact with uncoated cast iron may cause decohesion at the matrix-reinforcing phase boundary in places with weaker wetting of the surface of the particles with liquid silumin, which results in the removal of these particles, leaving traces with dimensions similar to the average diameter of the particles (**Fig. 8a**). No such traces were observed on the surface of the composite after sliding against the composite coating.

A comparison of the weight loss and coefficient of friction graphs clearly shows that the ceramic reinforcing phase in the chromium coating

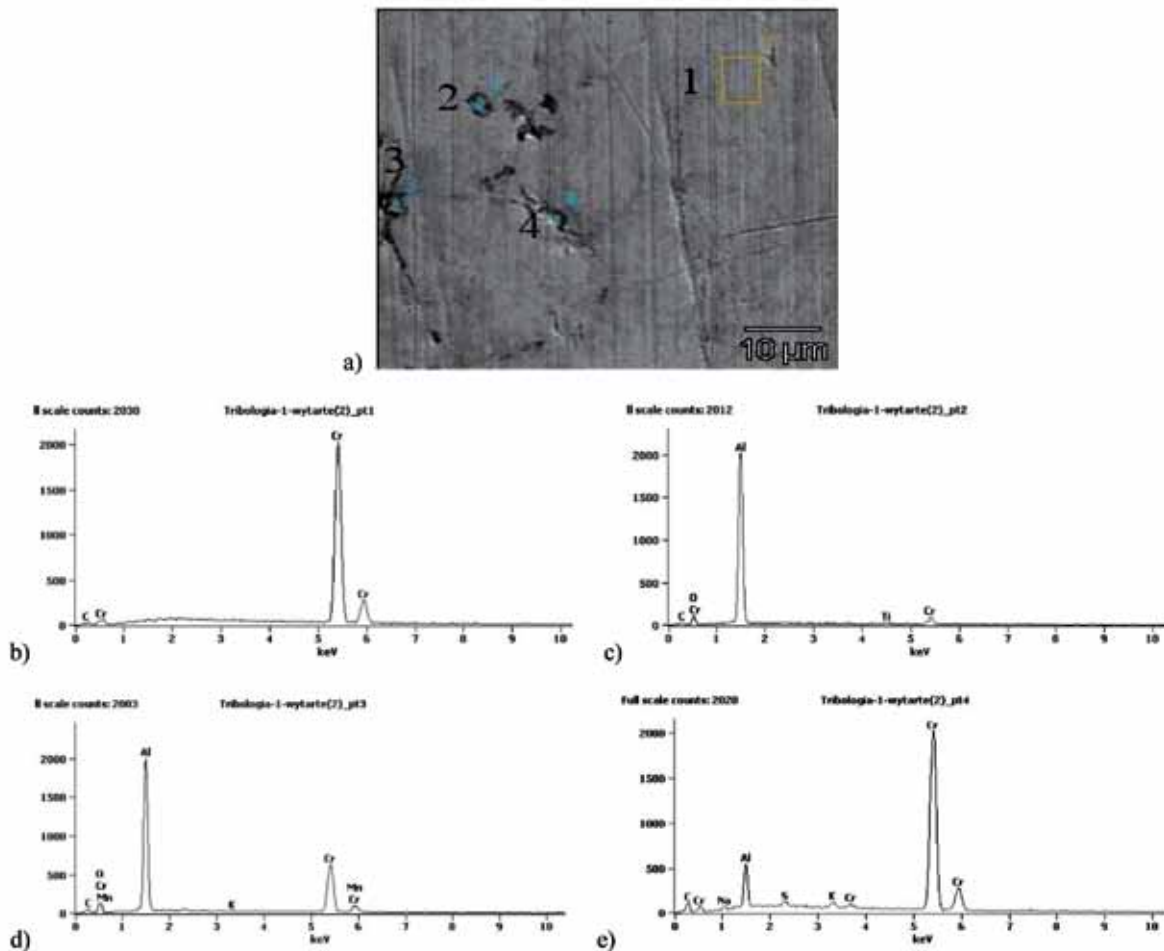


Fig. 9. Chemical composition of friction surface of GJL-250+Cr- Al_2O_3 ring after sliding against AIMC
Rys. 9. Skład chemiczny powierzchni roboczej pierścienia GJL-250+Cr- Al_2O_3 po współpracy z AIMC

accelerates running-in, reducing friction forces and wear in contact with the silumin matrix composite also containing Al_2O_3 particles.

CONCLUSIONS

Based on the results of the conducted research, the following conclusions can be drawn:

- The Cr- Al_2O_3 composite coating, deposited on cast iron piston rings, developed for sliding

against chromium-plated cylinder liners of internal combustion engines, is also suitable for sliding against silumin matrix composites reinforced with ceramic particles;

- The presence of Al_2O_3 particles and fibres in the chromium coating accelerates the running-in twofold, reducing the friction forces (about 20%) and wear (about three times) of the cast iron ring in contact with the silumin matrix composite also containing Al_2O_3 particles.

REFERENCES

1. Nakada M.: Trends in engine technology and tribology, *Tribology Internat.* 1994, Vol. 27 (1), pp. 3–8.
2. Posmyk A.: *Tribologia materiałów kompozytowych w pojazdach samochodowych*. Wyd. Politechniki Śląskiej Gliwice 2020.
3. Pędzich Z.: Zużycie abrazyjne kompozytów na osnowie tlenku glinu, *Kompozyty* 2007, 7(3), pp. 149–154.
4. Lubecki M., Stosiak M., Leśniewski T.: Comparative studies of tribological properties of selected polymer resins for use in hydraulic systems, *Tribologia* 2019, 6, pp. 31–37.
5. Linsmeier K-D.: *Technische Keramik Werkstoff für höchste Ansprüche*, Verlag Moderne Industrie Landsberg/Lech 2010.
6. Posmyk A.: Kształtowanie właściwości tribologicznych warstw wierzchnich tworzyw na bazie aluminium. Z. 62. *Hutnictwo*, Wydawnictwo Politechniki Śląskiej, Gliwice 2002.
7. Łuszcz M., Michalczewski R., Kalbarczyk M. at all: Effect of HBN on wear of AlCrN-coated spark plasma-sintered TiB₂/Ti composites at temperatures up to 900°C, *Tribologia* 2002, 1, pp. 43–55.
8. Posmyk A., Bąkowski H.: Wear mechanism of cast iron piston ring/aluminum matrix composite cylinder liner, *Tribology Transactions*, 56 (2013), pp. 806–815.
9. Łyziński M.: Pokrycia diamentowe pierścieni tłokowych, [http://old.intercars.com.pl/pliki/ INTER-CARS](http://old.intercars.com.pl/pliki/INTER-CARS), *Biuletyny Informacyjne* 2006, p. 61.
10. Kula P., Pietrasik R., Pawęta S., Komorowski J.: MoS₂/WS₂/fine LPN composite layers – a new approach to low frictional coatings for piston rings, *Tribologia* 2022, 3, pp. 49–58.
11. Kaźmierczak A.: *Tarcie i zużycie zespołu tłok-pierścienie-cylinder*, Oficyna Wydawnicza Politechniki Wrocławskiej, Wrocław 2005.
12. Kozaczewski W.: *Konstrukcja grupy tłokowo-cylindrowej silników spalinowych*, WKŁ, Warszawa 2004.
13. Zeyu M.A., Ruoxuan H., Xiaoshuai Y., Yan S., Jiujun X.: Tribological performance and scuffing behaviors of several automobile piston rings mating with chrome-plated cylinder liner, *Friction* 2022, 10 (8), 1245–1247.
14. Ruoxuan H., Zichun W., Xiaoshuai Y., Tianchi Z., Siqi M., Xiangnan Ch., Jiujun X.: Tribological performance of nano-diamond composites-dispersed lubricants on commercial cylinder liner mating with CrN piston ring, *Nanotechnology Reviews* 2020, 9, pp. 455–464.
15. Aruna S.T., Grips V.K., Selvi E.V., Rajam K.S.: Studies on electrodeposited nickel-yttria doped ceria composite coatings, *Journal of Applied Electrochemistry* 2007, 37(6), pp. 991–1000.
16. Ernst H.: *An interpretative review of 20th century machining and grinding research*, Techn Solve inc. Cincinnati (OH), 2003.